Available online at www.sciencedirect.com
SCIENCE DIRECT®
Materials Science and Engineering C 26 (2006) 751 – 755
MATERIALS SCIENCE & ENGINEERING C
www.elsevier.com/locate/msec

Effect of sliding velocity on capillary condensation and friction force in a nanoscopic contact

Pierre-Emmanuel Mazeran *

Laboratoire en Mécanique Roberval, Université de Technologie de Compiègne, BP 60319, 60206 Compiègne Cedex, France

Available online 28 October 2005

Abstract

The influence of sliding velocity on the friction force in a nanoscopic contact was studied on a hydrophilic silicon nitride surface with an Atomic Force Microscope. By submitting a nanoscopic contact to small oscillating lateral displacements, we observe both decreases of the friction force and of the contact radius with an increase of the sliding velocity. We found experimentally that this decrease of the friction force and of the contact radius is correlated to a decrease of the capillary force.

Keywords: Scanning force microscope; Sliding friction; Velocity; Capillary force

1. Introduction

Friction is an everyday life issue in industrial processes and natural phenomena [1,2]. It is involved in a great variety of fields like for example, granular media, earthquake dynamics or Micro ElectroMechanical Systems (MEMS). Nevertheless, the fundamental understanding of friction at the nanometer scale is actually too poor in front of the scientific and technological stakes. From a technological point of view, the development of nanotechnologies leads to the miniaturization of moving components for which the surface interactions (adhesion, friction and wear) become of primary importance. The development of Atomic Force Microscopy (AFM) has opened new possibilities for investigations of friction, adhesion and wear at nanometer scale [3]. The sliding velocity dependence of friction has been studied leading to contradictory results: Logarithmic increases or decreases of friction with the sliding velocity have been reported [4–8]. Recently Riedo et al. [8] suggested that the logarithmic dependence of friction to sliding velocity was due to two opposite phenomena. The first one is due to stick–slip motion, which gives a logarithmic increase of friction with an increasing sliding velocity [4,6]. The second one is due to the kinetics of capillary condensation of water vapor around the contact area, which causes a logarithmic decrease of the friction with an increasing sliding velocity [8].

2. Capillary condensation

When two surfaces are close together in the presence of a vapor under saturation, water (or any other liquid) may condense to form a liquid bridge between the two surfaces [9]. At the equilibrium, the surface curvature of the meniscus is imposed by the Kelvin radius R_K:

$$\frac{1}{R_K} = \frac{1}{R_{Min}} + \frac{1}{R_{Max}} \quad (1)$$

where R_{Min} and R_{Max} are the minimum and maximum curvature radius of the meniscus. In the case of a meniscus between two parallel solid surfaces, the curvature radius is minimum ($R_{Min}<0$) along the planes perpendicular to the solid surfaces and maximum ($R_{Max}>0$) along the planes parallel to the solid surfaces (Fig. 1). When the meniscus increases in size, R_{Max} tends to infinity and R_{Min} tends to the Kelvin radius: The maximum height of this capillary bridge is then twice the Kelvin radius. At fixed temperature T, the Kelvin radius depends only of the relative humidity H:

$$R_K = -\frac{\gamma_{LV} V_L}{RT \log H} \quad (2)$$

* Tel.: +33 344 235 228; fax: +33 344 235 229.
E-mail address: mazeran@utc.fr.

0928-4931/$ - see front matter © 2005 Elsevier B.V. All rights reserved.
doi:10.1016/j.msec.2005.09.055

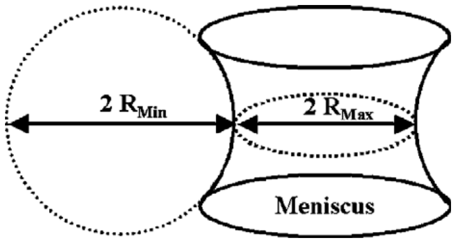

Fig. 1. Surface curvature of a capillary meniscus. A minimum curvature ($R_{\mathrm{Min}}<0$) and a maximum curvature radius ($R_{\mathrm{Max}}>0$) describe the surface curvature of the meniscus. The average curvature radius of the meniscus is equal to the Kelvin radius (R_{K}): $R_{\mathrm{K}}^{-1}=R_{\mathrm{Min}}^{-1}+R_{\mathrm{Max}}^{-1}$.

where γ_{LV} is the surface tension, V_{L} is the molar volume and R is the universal gas constant. The difference in pressure Δp between the liquid and its vapor is then:

$$\Delta p = \frac{\gamma_{\mathrm{LV}}}{R_{\mathrm{K}}}. \tag{3}$$

Fogden and White [10] and independently Maugis [11] have investigated the influence of the capillary force on an elastic sphere/sphere contact. They found that, for rigid materials, the depression inside the meniscus was too low to influence the geometry of the contact, which remains Hertzian [12]. The capillary force F_{C} just acts as an extra load that adds to the applied load F_{A} as suggested by Derjaguin et al. [13]. The total applied load F_{T} is then the sum of the applied load F_{A}, the capillary force F_{C} and others forces like for example the van der Waals force F_{vdW}. The capillary force F_{C} is proportional to the wet area A_{W}:

$$F_{\mathrm{C}} = A_{\mathrm{W}}\Delta p = A_{\mathrm{W}}\frac{\gamma_{\mathrm{LV}}}{R_{\mathrm{K}}}. \tag{4}$$

For a contact between two flat spheres, the ratio $A_{\mathrm{W}}/R_{\mathrm{K}}$ and then the capillary force is independent of the relative humidity and is equal to

$$F_{\mathrm{C}} = 4\pi R\ \gamma_{\mathrm{LV}}\cos\theta \tag{5}$$

where R is the radius of the sphere and θ is the static water contact angle of the meniscus. This equation is misleading in a nanoscopic contact, because the surface (typically in the nanometer range) is generally high compared to both the Kelvin radius and the indentation depth. Few publications clearly show that the capillary force is highly dependent on the relative humidity. Typically, for hydrophilic rough surface, the capillary force is maximum for a relative humidity of 20–40% [14,15].

Capillary condensation is a thermally activated process. It has been shown that for a constant relative humidity, the cohesion force of a granular media, by means of the maximum stability angle, is time-dependent [16,17]. The maximum height of water meniscus is twice the Kelvin radius. The Kelvin radius is in the nanometer range, for a relative humidity of 30% the Kelvin radius is equal to 1 nm. Water can only condense in nanometer-scale interstices or around the contact points. The presence of asperities on the two surfaces in contact generates nucleating sites for capillary bridges. At a given rest time only an increasing fraction of them is formed: The capillary force, which is proportional to the wet area, increases (Fig. 2). When sliding occurs, the residence time depends of the sliding velocity and then the wet area and the capillary force decreases with the sliding velocity [8]. Nevertheless, only little evidences of the decrease of the capillary force with the sliding velocity have been pointed out [15]. The aim of this paper is to show experimental evidences of the decrease of the capillary force with an increasing sliding velocity. We first investigated the nature of the contact. We show that in our experimental conditions, the roughness of the surface is small in front of the indentation depth and that the contact is close to a single asperity contact. Then, we investigated the friction dependence to velocity. Experimental results show that the friction force and the contact radius decrease with an increasing velocity. We demonstrate that the decreases are the result of a decrease of the capillary force. At last, we will show a direct evidence of the decrease of the capillary force with an increasing velocity.

3. Experiments

Experiments were performed with a commercial Atomic Force Microscope in contact mode (Dimension 3100, Nanoscope IIIa from Digital Instruments). Silicon nitride probes were used (DNP, Digital Instruments), the nominal curvature radius of the probe is 20 nm and the nominal stiffness of the cantilever is 0.58 N/m. The probe was brought in contact with the surface of a silicon nitride cantilever chip. The probe and sample surfaces have the same chemical and mechanical properties. The mechanical properties of the silicon nitride were measured by nanoindentation (Nanoindentor XP, MTS Systems). The hardness is equal to 25 GPa and the elastic modulus is equal to 140 GPa in good agreement with the literature [18]. The surface is hydrophilic, the water angle is equal to 30°. Experiments were performed under lab conditions. The relative humidity (typically 50–60%) was measured

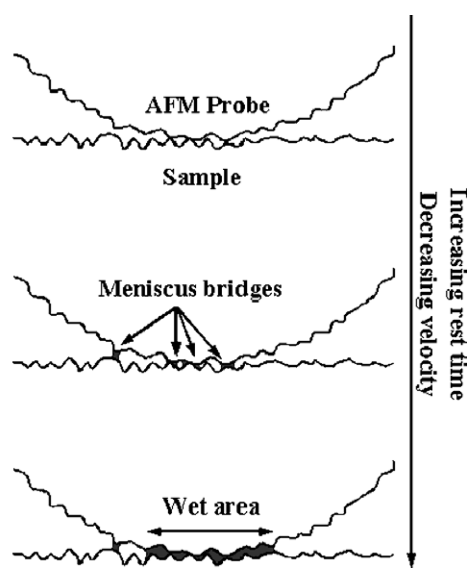

Fig. 2. Schematic of capillary water bridges formed in the contact area. The asperities of the surface act as nucleating site for capillary condensation. When the rest time increases, the wet area and then the capillary force increases.

using a commercial hygrometer. The AFM was modified for the tribological studies [19]: a lock-in amplifier generates a sinusoidal voltage at a typical frequency of a few kHz in order to generate a sinusoidal displacement of the probe parallel to the surface sample. The lateral force generated by this lateral displacement of the probe was analyzed by the lock-in amplifier and the in-phase and out-of-phase part of the lateral force was recorded. The calibration of the lateral displacement and the lateral force at these high frequencies is particularly difficult leading to a high uncertainty of the data.

3.1. Nature of the contact

To explain theirs experimental results, several authors [8,20] suggest that the contact between the probe and the sample was a polyasperities contact rather than a single asperity contact (Fig. 1). Nevertheless, the determination of the exact nature of the contact (single asperity or polyasperities contact, elastic or plastic contact) is particularly difficult and depends highly of the sample roughness. As a first approach, we consider that the contact in our experimental conditions follows the Hertz Theory. This theory gives the relation between the applied load, contact radius, indentation depth and contact pressure for an elastic contact between a flat sphere and a flat plane [12]. The plasticity and roughness of the surface are two obstacles to the validity of the Hertz theory. The theoretical average contact pressure was computed to be about 3 GPa. This value is small in front of the hardness of the sample (25 GPa) and we can conclude that the contact is theoretically elastic. To investigate the influence of the roughness, we propose to compare the roughness of the theoretical contact area to the theoretical indentation depth. If the theoretical indentation depth is high compared to the total roughness, we can conclude that the asperities are flattened out and that the contact remains Hertzian. On the other hand, if the theoretical indentation depth is small compared to the total roughness, we can conclude that the asperities are not flattened out and that the contact is a polyasperities contact (Fig. 3).

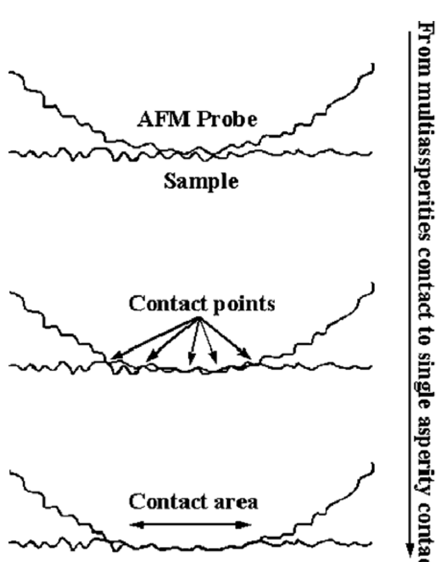

Fig. 3. Schematic of the transition from a polyasperities contact to a single asperity contact. As the applied load increases, the contact pressure flattens the asperities: The contact follows the Hertz theory.

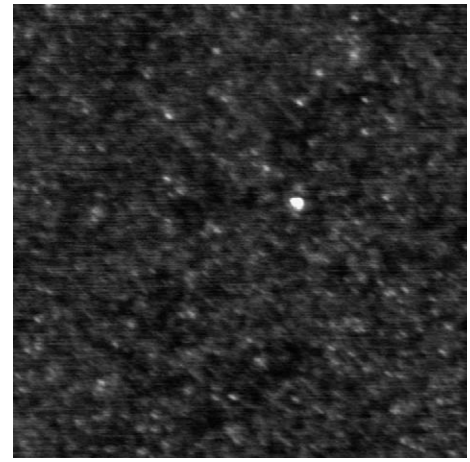

Fig. 4. 1 μm^2 scale topographic image of the silicon nitride sample (Z scale: 3 nm).

In a first time, we realized a topographic image of the silicon nitride sample (Fig. 4) using the so-called Tapping mode and a sharp silicon probe (MPP 11100 from Digital instruments). The nominal radius of the probe is 10 nm. In a second time we computed the peak-to-valley roughness for the whole image and decreasing fractions of it (quarter, 16th, 64th…). The peak-to-valley roughness of the fractions of the image is plotted in Fig. 5 as a function of their area. Using the Hertz theory, the indentation depth $\delta = A/\pi R$ is plotted on the same graph as a function of the contact area A. The graph shows that the theoretical indentation depth is superior to the roughness of the contact area for a contact area of about 12 nm^2. From Hertz, we can estimate the load corresponding to this area at approximately 60 nN. This force is of the same order than the total applied load (typically 50 nN). Because the roughness in the contact area is a statistical event, we conclude that the

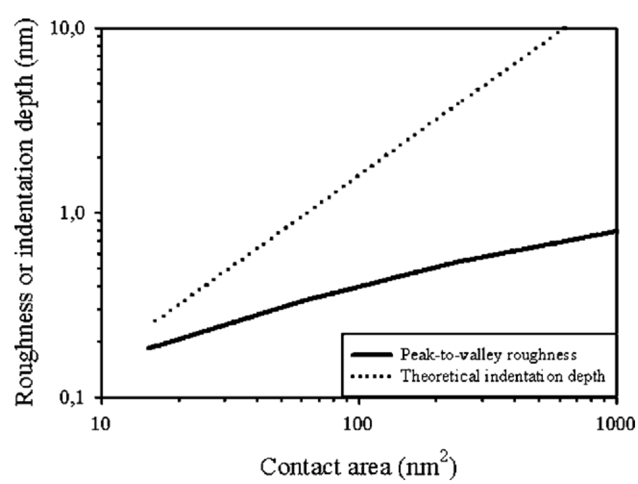

Fig. 5. Comparison between the peak-to-valley roughness of the silicon nitride sample and the theoretical indentation depth as a function of the contact area. We observe that the indentation depth is high compared to the peak-to-valley roughness. The asperities are flattened out and the contact may obey the Hertz law.

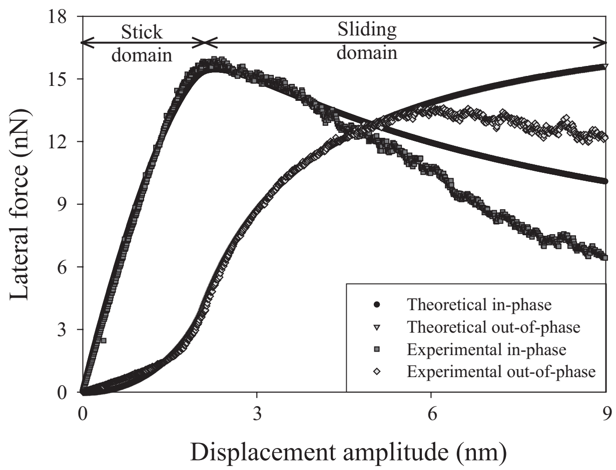

Fig. 6. Comparison between the experimental and the theoretical in-phase and out-of-phase part of the lateral force as the function of the displacement amplitude (velocity). At high displacement amplitude, we observe a decrease of both the experimental in-phase and out-of-phase component of the lateral force compared to the theoretical values. This result is interpreted as a decrease of the attractive force.

contact is mainly Hertzian but that the presence of asperities could lead locally to a poly asperities contact.

3.2. Friction dependence of the velocity

We investigated the friction dependence to the sliding velocity using the following set-up. For a constant applied load (10 nN), we generated a sinusoidal lateral displacement d of this single asperity contact at a frequency of 6135 Hz. This frequency corresponds to a resonance of the AFM piezo scanner. The amplitude of the lateral displacement increased linearly with time from zero to a few tens of nanometer and then decreases linearly to zero during a period of about 2 min. The lateral force generated by the lateral displacement was analyzed by the lock-in amplifier and the in-phase and out-of-phase part of the lateral force is plotted as a function of the amplitude of the lateral displacement (Fig. 6). The in-phase part of the lateral force is proportional to the ratio between the energy stored during one cycle and the displacement length. This energy is principally due to shear of the contact. The out-of-phase part of the lateral force is proportional to the ratio of the energy dissipated to the displacement length. This energy is principally dissipated by friction. We used the Mindlin theory [21,22] as a model for our experiments. This theory describes the increase of the lateral force as a function of the relative displacement of a contact. This model is based on a Hertz contact with a linear dependence of the friction force to the total applied load. In our experimental conditions, the total applied load is the sum of the applied load, capillary force and van der Waals force. While the amplitude of the lateral displacement is low in front of the contact radius, the contact is principally sheared and sliding occurs only in the periphery of the contact: We are in the stick domain. The in-phase part of the lateral force is then far higher than the out-of-phase part of the lateral force. When the amplitude of the lateral displacement becomes high compared to the contact diameter, the energy is mainly dissipated by fiction: We are in the sliding domain. The out-of-phase part of the lateral force becomes higher than the in-phase part of the lateral force.

Experimental results were fitted with the Mindlin model by adjusting two parameters: the contact radius and the friction force (Fig. 6). For lateral displacement amplitudes below approximately 5 nm, A very good agreement is observed between theoretical and experimental results. Beyond this value, the in-phase and out-of-phase contribution to the lateral force become quite lower than the theoretical values. This result is an evidence of the decreases of the elastic energy stored in the contact and the energy dissipated by friction. In the Mindlin model, the elastic energy stored in the contact as well as the energy dissipated by friction are proportional to the total applied load. It becomes then obvious that the total applied load decreases as the lateral displacement amplitude increases. There is a direct relation between the displacement amplitude and the maximum velocity $V=2\pi fd$ during an experiment. We conclude that the total applied load decreases as the sliding velocity increases. The applied load was maintained constant during the experiment, then we may conclude that this is the attractive force, the sum of the capillary and the van der Waals force, that decreased during the experiment.

3.3. Adhesion force dependence on friction

To confirm the previous experiments, we measured the adhesion force as a function of the sliding velocity of the probe. A sinusoidal lateral displacement of the probe was generated at a fixed frequency f with an amplitude d. The normal applied force is plotted as a function of the probe/surface distance in Fig. 7. While the total applied load (sum of the normal applied load and attractive force) is greater than zero, the probe is in contact with the surface. When the probe snaps off the surface, the absolute value of the applied load is equal to the attractive force. We define this force as the adhesive force, sum of capillary and van der Waals when the probe leaves the surface.

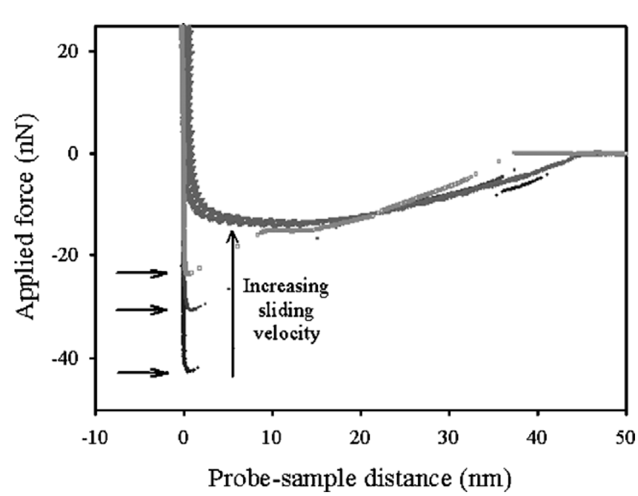

Fig. 7. Force as a function of the probe/sample distance for an increasing sliding velocity. We observe a decrease of the snap-off force (marked by arrows) with an increase of the velocity. This decrease is the result of the decrease of the capillary force.

We observed a decrease of the adhesive force with an increase of the maximum sliding velocity. For a high value of the velocity, the force/distance curve looks like a Lennard–Jones force curve. We conclude that for an enough high sliding velocity of the probe, the capillary force vanishes with the absence of capillary condensation. The adhesive force recorded is then only due to a van der Waal interaction.

4. Conclusion

In conclusion, we showed that for a nanoscopic contact between hydrophilic surfaces, both the friction force and the contact radius decreases with the sliding velocity. These decreases have been explained experimentally by a decrease of the adhesive force with the sliding velocity due to the disappearance of the capillary force.

References

[1] E. Meyer, R.M. Overney, K. Dransfeld, T. Gyalog, Nanoscience: Friction and Rheology on the Nanometer Scale, World Scientific, Singapore, 1998.
[2] B. Bhushan, Micro/Nanotribology and its Applications, Kluwer Academic Publishers, Dordrecht, 1997.
[3] R.W. Carpick, M. Salmeron, Chem. Rev. 97 (1997) 1163.
[4] T. Bouhacina, J.P. Aimé, S. Gauthier, D. Michel, V. Heroguez, Phys. Rev., B 56 (1997) 7694.
[5] O. Zwörner, H. Holscher, U.D. Schwarz, R. Wiesendanger, Appl. Phys., A 66 (1998) S263.
[6] E. Gnecco, R. Bennewitz, T. Gyalog, C. Loppacher, M. Bammerlin, E. Meyer, J. Güntherodt, Phys. Rev. Lett. 84 (2000) 1172.
[7] H. Liu, S.I.U. Ahmed, M. Scherge, Thin Solid Films 381 (2001) 135.
[8] E. Riedo, F. Lévy, H. Brune, Phys. Rev. Lett. 18 (2002) 185505.
[9] J. Israelachvili, Intermolecular and Surface Forces, Academic Press, San Diego, 1977.
[10] A. Fogden, L.R. White, J. Colloid Interface Sci. 138 (1990) 414.
[11] D. Maugis, J. Colloid Interface Sci. 150 (1992) 243.
[12] H. Hertz, J. Reine Angew. Math. 92 (1882) 156.
[13] B.V. Derjaguin, V.M. Muller, Y.P. Toporov, J. Colloid Interface Sci. 53 (1975) 314.
[14] M. He, A. Szuchmacher Blum, E. Aston, C. Buenviaje, R. Overney, J. Chem. Phys. 14 (2001) 1355.
[15] L. Sirghi, Appl. Phys. Lett. 82 (2003) 3755.
[16] F. Restagno, C. Ursini, H. Gayvallet, E. Charlaix, Phys. Rev., E 66 (2002) 021304.
[17] L. Bocquet, E. Charlaix, S. Ciliberto, J. Crassous, Nature 396 (1998) 735.
[18] J.E. Sader, I. Larson, P. Mulvaney, L.R. White, Rev. Sci. Instrum. 66 (1995) 3789.
[19] P.E. Mazeran, J.L. Loubet, Tribol. Lett. 7 (1999) 199.
[20] N.S. Tambe, B. Bhushan, J. Phys., D 38 (2005) 764.
[21] R.D. Mindlin, Trans. ASME, Ser. E, J. Appl. Mech. 16 (1949) 259.
[22] R.D. Mindlin, W.P. Mason, F. Osmer, H. Deresiewicz, Proc. 1st US National Congress of Applied Mechanics, New York, United States, 1954, p. 203.